

Article

Application of Analytic Hierarchy Process in Mineral Prospecting Prediction Based on an Integrated Geology-Aerogeophysics-Geochemistry Model

Yongzai Xi ^{1,2,3}, Yongbo Li ^{1,2,3} , Junjie Liu ^{1,2,3}, Shan Wu ^{1,2,3}, Ning Lu ^{1,2,3,*} , Guixiang Liao ^{1,2,3,*} and Qiule Wang ^{1,2,3}

- ¹ Institute of Geophysical and Geochemical Exploration, Chinese Academy of Geological Sciences (CAGS), Langfang 065000, China; xyongzai@mail.cgs.gov.cn (Y.X.); lyongbo@mail.cgs.gov.cn (Y.L.); ljunjie@mail.cgs.gov.cn (J.L.); wshan@mail.cgs.gov.cn (S.W.); wqiule@mail.cgs.gov.cn (Q.W.)
- ² Key Laboratory of Geophysical Electromagnetic Probing Technologies, Ministry of Natural Resources (MNR), Langfang 065000, China
- ³ National Center for Geological Exploration Technology, Langfang 065000, China
- * Correspondence: luning@mail.cgs.gov.cn (N.L.); lguixiang@mail.cgs.gov.cn (G.L.)

Abstract: Determining mineral prospecting targets is crucial for mineral prediction and evaluation. In this study, an evaluation index system for solid mineral exploration and metallogenic target assessment was established using the Analytic Hierarchy Process (AHP) for the Naoniushan area (China). Furthermore, an integrated model combining geology–aerogeophysics–geochemistry was developed for copper, lead, zinc, silver, and other polymetallic deposits. The information content of each index in the model was reasonably assigned, and the mineral prospecting targets in the central and southern parts of the Daxinganling were recommended. By focusing on the copper polymetallic mineral prospecting target in the Naoniushan area, this paper demonstrates that the AHP method can comprehensively consider various influencing factors and their interactions, realize a reasonable division of the optimal mineral prospecting target, and reflect the key factors affecting the mineral prospecting target to a certain extent. Importantly, this approach reduces the influence of human subjective factors, and the optimization results are objective and scientifically grounded.

Keywords: analytic hierarchy process (AHP); integrated model; information entropy method; prospecting target area; Naoniushan area



Citation: Xi, Y.; Li, Y.; Liu, J.; Wu, S.; Lu, N.; Liao, G.; Wang, Q.

Application of Analytic Hierarchy Process in Mineral Prospecting Prediction Based on an Integrated Geology-Aerogeophysics-Geochemistry Model. *Minerals* **2023**, *13*, 978. <https://doi.org/10.3390/min13070978>

Academic Editor: Behnam Sadeghi

Received: 25 June 2023

Revised: 21 July 2023

Accepted: 21 July 2023

Published: 23 July 2023



Copyright: © 2023 by the authors. Licensee MDPI, Basel, Switzerland. This article is an open access article distributed under the terms and conditions of the Creative Commons Attribution (CC BY) license (<https://creativecommons.org/licenses/by/4.0/>).

1. Introduction

In recent years, extensive airborne geophysical exploration has been conducted in the central and southern sections of the Daxinganling Mountains, covering approximately 250,000 line kilometers. This survey provided valuable basic data for mineral exploration and geological research in the region. One of the key challenges we face is how to effectively utilize the existing geological, airborne geophysical, and geochemical data to define prospecting target areas for polymetallic mineralization in this area.

Quantitative methods can be employed to establish a mineralization model based on the comprehensive geological, geophysical, and geochemical conditions of known deposits. Analogies can be used for quantitative calculations and anomaly classification. However, this approach is only applicable to areas with a high level of work. In cases where the data are insufficient and the model's assumptions are violated due to incomplete or missing values of the explanatory variables in the study area, the model cannot be applied. Additionally, if multicollinearity is present, the standard deviation of the regression coefficients will increase, rendering the model unreasonable [1–4]. On the contrary, qualitative methods are not as highly dependent on work level as quantitative methods, but there is much uncertainty due to different perceptions by different researchers [5–9].

The Analytic Hierarchy Process is a commonly used method for solving problems related to the comprehensive evaluation of multiple factors. It combines qualitative and quantitative methods to decompose mineralization prediction problems into several key influencing factors that judge the likelihood of mineralization and form a hierarchical structure according to their dominant relationships. The prospecting target areas can be determined through pairwise comparisons, and previous researchers have achieved good results. Wang et al. validated the effectiveness of the Analytic Hierarchy Process in uranium mineralization prediction in the Tarim Basin, China. Hao et al. applied this method in the Puqing mining area in Guizhou, China, and successfully identified 18 prospective areas for antimony (gold) mineralization. The exploration and verification results demonstrated the objectivity and effectiveness of this method. Ali et al. applied the Fuzzy- Analytic Hierarchy Process method in eastern Iran and obtained comprehensive metal mineralization prospective areas [10–16].

In this study, we constructed a complete evaluation index system by considering the characteristics of airborne geophysical exploration and combining geological and geochemical data. We calculated the relative weights of each indicator to form a scoring standard for the geological–airborne geophysical–geochemical integrated model. We also produced an information entropy contour map of the model, providing a sufficient basis for delineating the target areas.

2. Analytic Hierarchy Process

The Analytic Hierarchy Process (AHP) method was initially proposed by T.L. Saaty, an American operations researcher and professor at the University of Pittsburgh, in the early 1970s [17]. This method can digitize personal experience and thinking, realizing a combination of qualitative and quantitative methods, and has been widely applied in various fields [18–31]. In this study, the AHP was employed to break down mineralization prediction problems into several ore-controlling factors that influence the mineralization probability (such as known geological, geophysical, and geochemical characteristics) and establish an objective hierarchical analysis model for mineral exploration. According to previous researchers' summarized mineralization theories and experiences, relative importance comparisons were made for each level and factor, assigning numerical values accordingly. The weight values of each level and factor were calculated using mathematical methods, and the mining target areas were predicted based on identifying mineralization anomalies and expected anomalies. This approach offers the potential for obtaining favorable geological exploration outcomes. The modeling process using AHP can be divided into the following four steps [6]:

2.1. Establishing an AHP Model

When utilizing AHP to analyze decision-making problems, the first step involves organizing and hierarchizing the problem and constructing a hierarchical structure model. Under this model, complex problems are decomposed into several levels and analyzed gradually in levels that are much simpler than the original to solve complex problems. The number of levels in this hierarchical structure depends on the complexity of the problem and the level of detail required for analysis. Generally, there is no set limit to the number of levels. However, it is recommended that each element in each level not dominate more than nine other elements to avoid difficulties in pairwise comparison and judgment caused by a large number of elements. A sound hierarchical structure is extremely important for solving problems. Therefore, it must be built on the decision-maker's comprehensive and thorough understanding of the problem. The interrelationships between the elements must be clarified to ensure the establishment of a reasonable hierarchical structure.

2.2. Constructing Judgment Matrices and Scales

Evaluating level A using a judgment matrix involves comparing the relative importance of factors B1, B2, . . . , and Bn in the next level B. This comparison is typically expressed in the following form (Table 1).

Table 1. The general form of a judgment matrix.

A	B1	B2	...	Bn
B1	B1/B1	B1/B2	...	B1/Bn
B2	B2/B1	B2/B2	...	B2/Bn
⋮	⋮	⋮	⋮	⋮
Bn	Bn/B1	Bn/B2	...	Bn/Bn

To quantify the judgment matrix, Saaty et al. suggested using the numbers one to nine and their reciprocals as the scale [17]. Table 2 shows the meanings associated with the scale values one to nine.

Table 2. The meaning of judgment matrix scale.

Scale	Meaning
1	Two elements are compared; both elements have equal importance.
3	Two elements are compared; the former is slightly more important.
5	Two elements are compared; the former is significantly more important.
7	Two elements are compared; the former is strongly important.
9	Two elements are compared; the former is extremely important.
2, 4, 6, 8	Represent the median values of the adjacent judgments mentioned above.

2.3. Single-Level Ranking Weights and Consistency Testing

Based on the judgment matrix obtained, the weight can be calculated by determining the maximum eigenvalue and eigenvector. Then, the maximum weight vector is normalized and outputted. Due to the complexity of objective matters and the diversity of human cognition, a consistency test is conducted at the conclusion to ensure judgments align with common sense. The steps of the consistency test are as follows [9]:

1. Calculate the consistency index C_I

$$C_I = \frac{\lambda_{max} - n}{n - 1}$$

where λ_{max} is the maximum eigenvalue of the judgment matrix, and n is the order of the judgment matrix.

2. Look up the corresponding average consistency index R_I .

The average random consistency index R_I gives the average consistency index obtained by calculating 1000 samples with a matrix of positive reciprocal values ranging from one to nine, as illustrated in Table 3.

Table 3. Average random consistency index.

n	1	2	3	4	5	6	7	8	9
R_I	0	0	0.52	0.89	1.12	1.26	1.36	1.41	1.46

3. Calculate the consistency ratio C_R .

$$C_R = \frac{C_I}{R_I}$$

Based on Formulas (1) and (2), the value of C_I can be calculated. When C_I is less than 0.10, the consistency of the judgment matrix is considered acceptable. Otherwise, appropriate adjustments should be made to the judgment matrix.

2.4. Calculation of the Total Hierarchy Ranking Weights

If the upper-level A contains m factors, namely A_1, A_2, \dots, A_m , with corresponding total hierarchical ranking weights of a_1, a_2, \dots, a_m , and the lower-level B contains n factors, namely B_1, B_2, \dots, B_n , and their single-level ranking weights for factor A_j denote as $b_{1j}, b_{2j}, \dots, b_{nj}$ (if B_k is not related to $A_j, b_{kj} = 0$), then the total hierarchy ranking weights of level B can be obtained according to the information provided in Table 4.

Table 4. Calculation table sorting weight of hierarchy.

B \ A	A	A_1	A_2	...	A_m	Total Hierarchy Ranking Weights of Level B
		a_1	a_2	...	a_m	
B_1		b_{11}	b_{12}	...	b_{1m}	$\sum_{j=1}^m b_{1j}a_j$
B_2		b_{21}	b_{22}	...	b_{2m}	$\sum_{j=1}^m b_{2j}a_j$
\vdots		\vdots	\vdots	\vdots	\vdots	\vdots
B_n		b_{n1}	b_{n2}	...	b_{nm}	$\sum_{j=1}^m b_{nj}a_j$

The relative importance weight of level C with respect to the overall goal can also be obtained using the matrix scale and calculation method mentioned earlier.

3. The Construction and Weight of the Evaluation Index System

3.1. The Construction of the Evaluation Index System

The purpose of the evaluation is to make valuable judgments regarding the evaluated object. Therefore, establishing an evaluation index system for the optimal selection of mineral exploration target areas should provide a specific and operational evaluation index system. The establishment of this index system needs to determine the overall goal, establish the goal layer, decompose the overall goal into a primary index system, a secondary index system, and so on. This ultimately forms the evaluation general system table.

According to the geological purpose of this study, polymetallic ores such as copper, lead, zinc, and silver are the prediction targets of airborne geophysical anomalies. By examining mineral exploration indicators possessed by geological, airborne geophysical (magnetic, radiometric, electromagnetic), and geochemical data, a hierarchical analysis conceptual model of airborne geophysical anomaly prediction and evaluation is shown in Figure 1. The model consists of two levels. The first level is the purpose level (A), representing the model’s objective to delineate the mineralized target areas. The second level is the criterion level (B, C), which includes three main levels: geological, airborne geophysical, and geochemical comprehensive evaluation (B) and eight specific evaluation indicators of sub-levels (C).

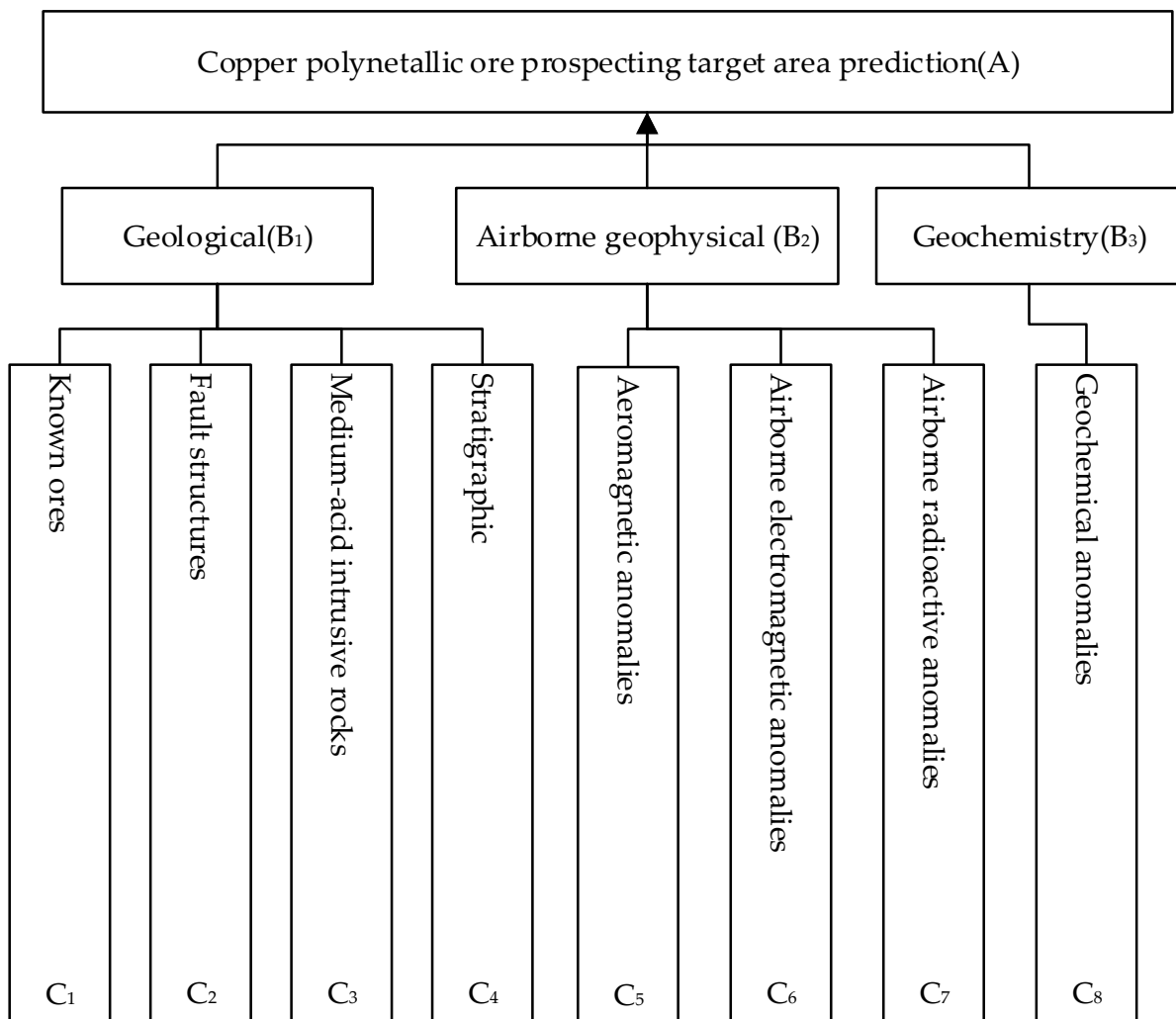


Figure 1. Conceptual model of hierarchical analysis for the prediction of copper polymetallic ores.

1. Geological signs (B_1)

- (1) Known ores (C_1): summarizing the information about known ore deposits and mineralization points is the primary sign for predicting the mineralized target area.
- (2) Fault structures (C_2): according to regional geological data, the fault and structural signs in the area include intersections of two or more faults and single faults.
- (3) Medium-acid intrusive rocks (C_3): medium-acid intrusive rocks are widely distributed in the area, can be found in the form of rock stocks, branches, and bases, and are closely related to endogenous mineralization. Most of the mineral deposits in the area are distributed in Permian and Jurassic intrusive rocks, which serve as the primary ore-forming parent rocks in the area. The contact zone between the rock bodies and the surrounding rocks is considered a favorable position for mineralization.
- (4) Stratigraphic (C_4): the statistical distribution of known ores shows that the favorable stratigraphic layers for copper polymetallic ores are the Upper Jurassic and Lower Permian.

2. Airborne geophysical signs (B_2)

- (1) Aeromagnetic anomalies (C_5): anomalies that are closely related to known mineralization, anomalies inferred to be related to mineralization, anomalies with

unclear properties, and anomalies inferred to have low exploration significance based on existing data.

- (2) Airborne electromagnetic anomalies (C₆): anomalies inferred to be mineralized alteration zones or mineralized fault zones; anomalies inferred to be fault fracture zones; anomalies inferred to be low-resistivity rock; or anomalies with unclear properties.
- (3) Airborne radiometric anomalies (C₇): two types of anomalies, namely potassic alteration zone anomalies and uranium and thorium anomalies.

3. Geochemical anomalies (B₂)

According to the collected soil geochemical data from the 1:200,000 scale survey, the main ore-forming elements related to copper polymetallic ores are Ag, Cu, Au, and Zn. The characteristics of anomalous element content, scale, and concentration zoning are important signs for direct mineral exploration (C₈).

3.2. Determination of Evaluation Index Weights

According to the principle of the AHP, two pairwise comparison matrices were constructed for the primary and secondary indicators of the evaluation index system for the optimal selection of mineral exploration target areas. The final discrimination matrix was obtained by numerical transformation, and its maximum eigenvalue and weight vector were calculated. Then, a consistency check was performed to finally determine the weight of each indicator and establish the information entropy evaluation model table based on the weight values, as shown in Tables 5 and 6.

Table 5. Initial weighted value of each evaluation index.

Evaluation Contents	Initial Weights	Evaluation Indicators	Initial Weights
Geological	0.5	Known ores	0.20
		Stratigraphic	0.10
		Medium-acid intrusive rocks	0.10
		Fault structures	0.10
Airborne geophysical	0.3	Aeromagnetic local anomalies	0.14
		Airborne electromagnetic local anomalies	0.08
		Airborne radiometric local anomalies	0.08
Geochemical	0.2	Geochemical anomalies	0.20

Table 6. Table of models for comprehensive information evaluation of geology—aerogeophysical and geochemical information.

Indicators	Assignment Signs	Values
Known ores (20 points)	Large, medium, and small-sized ore deposits Within 1 km of known ore deposits.	20
	Mineralization points Within 0.5 km of known mineralization points.	15
Geological (50 points)	Alteration of surrounding rocks.	10
	Ore-bearing stratigraphic layer. (P ₁ d ² , P ₁ t, P ₁ , P ₁ b, P ₁ z _s , P ₁ ds, P ₂ l, P ₁ g, P ₂ s, P ₁ w, P ₁ sh, P ₁ x)	10
	Ore-bearing stratigraphic layer. (O ₂ h, O ₁ w, D ₁ , D ₂ t, C ₂ b, C ₃ h ⁴ , D ₃ a, Tt ¹ , Tt ² , T ₁ h, S ₃)	8
	Ore-bearing stratigraphic layer. (J ₂ f, J ₂ h, J ₃ mn)	6
Stratigraphic (10 points)	Other stratigraphic layers.	4

Table 6. Cont.

Indicators	Assignment Signs	Values		
Medium-acidic intrusive rocks. (10 points)	Permian and Jurassic rocks	Rock stock or branch	Contact zone (within and outside 0.5 km). 10	
			Within rock stocks and branches. 8	
		Base rock		Contact zone (within and outside 0.5 km). 8
				Within rock bases. 6
	Other rocks	Rock stock or branch		Contact zone (within and outside 0.5 km). 6
				Within rock stocks and branches. 4
		Base rock		Contact zone (within and outside 0.5 km). 4
				Within rock bases. 2
	Fault structure (10 points)	Intersection of two or more faults.		10
		One fault		7
Airborne geophysical (30 points)	Aeromagnetical anomalies (14 points)	Anomalies closely related to known mineralization (Type A anomalies).		14
		Anomalies inferred to be related to mineralization (Type B anomalies).		10
		Anomalies with unclear properties (Type C anomalies).		6
		Anomalies inferred to have no exploration significance based on existing data (Type D anomalies).		4
	Airborne electromagnetic anomalies (8 points)	Anomalies inferred to be mineralized alteration zones or mineralized fault zones		8
		Anomalies inferred to be fault fracture zones		6
		Anomalies inferred to be low-resistivity rock or anomalies with unclear properties		4
	Airborne radiometric anomalies (8 points)	Potassic alteration zone anomalies		8
		Uranium and thorium anomalies.		6
	Geochemical (20 points)	Multi-element combination anomalies, there are two or more ore-forming elements with anomalous content of Cu, Pb, Zn, and Ag, at least one of which is an internal zone, and there are front-end element anomalies (one or more of As, Sb, and Hg); Cu, Mo, and Au with front-end element combination anomalies, and either Cu or Mo is in the internal zone.		20
Multi-element combination anomalies, there are one or more ore-forming elements with anomalous content of Cu, Pb, Zn, and Ag, at least one of which is in the middle zone, and there are front-end element anomalies (one or more of As, Sb, and Hg); Cu, Mo, and Au with front-end element combination anomalies, and either Cu or Mo is in the middle zone.		16		
Multi-element combination anomalies, there are two or more ore-forming elements with anomalous content of Cu, Pb, Zn, and Ag, at least one of which is in the middle zone or above, and there are tailing elements (one or more of W, Sn, Mo, and Bi) without front-end element anomalies; Cu, Mo, and Au combinations without front-end element anomalies; multi-element combination outer zone anomalies, i.e., there are ore-forming elements (one or more of Cu, Pb, Zn, and Ag) and front-end elements (one or more of As, Sb, and Hg).		12		
Multi-element combination outer zone anomalies, without front-end element (As, Sb, and Hg) anomalies; multi-element combination anomalies without ore-forming elements (Cu, Pb, Zn, and Ag); single-element anomalies in the middle zone or above.		8		
Any single-element outer zone anomaly.		4		

Note: The last column, "values" is an evaluation score, which is dimensionless data.

3.3. Weighting Method for Prediction Models

Using the above-established AHP comprehensive information prospecting model with a grid size of $2\text{ km} \times 2\text{ km}$, the entire area is divided into several equally sized grid units. The information values of each prospecting indicator within each grid unit are added up. The resulting comprehensive information value is used to contour the map, as shown in Figure 2. Finally, the minimum threshold for the prospecting area is determined by comparing the information values of the known mineralized areas.

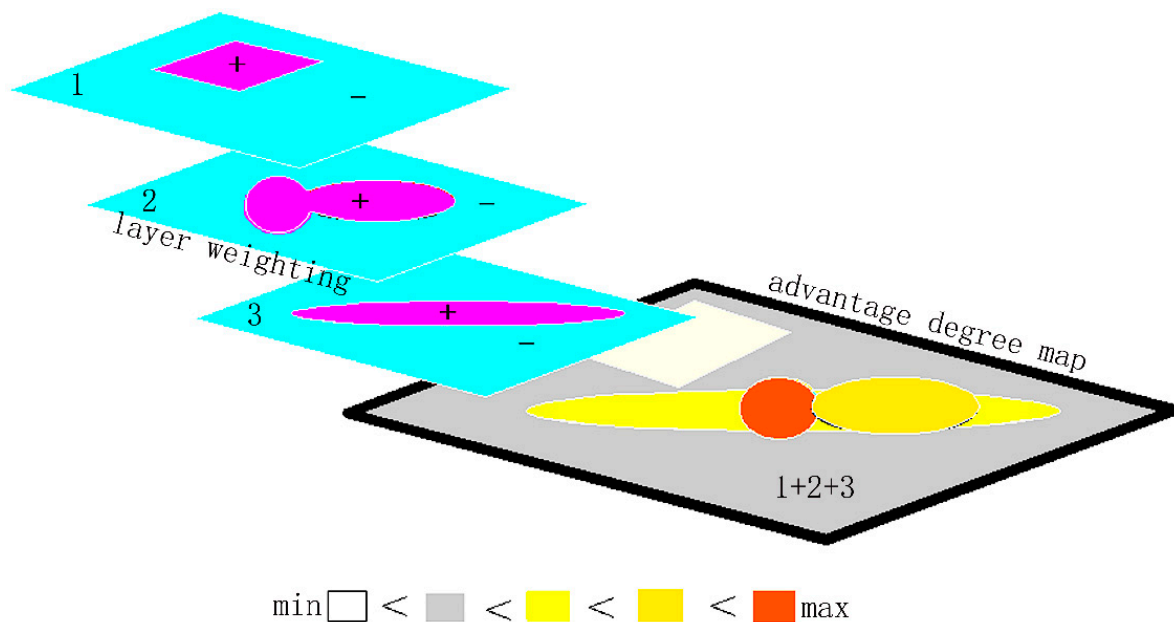


Figure 2. A schematic diagram of the algorithm of mark information in the metallogenic prospect area.

4. Application

The central–southern part of the Great Xing’an Range is characterized by the strong superposition, combination, and transformation of the Paleozoic Paleo-Asian Ocean tectonic metallogenic domain and the Cenozoic Binxian-West Pacific tectonic metallogenic domain. It exhibits the typical features of multiple accretionary orogenic belts. The endogenous metallic mineral resources in this area mainly include iron, copper, nickel, gold, silver, tin, lead–zinc, copper–zinc, copper–lead, lead–zinc–silver, iron–polymetallic, and copper–polymetallic mineral deposits. According to different genetic types, the known deposits (points) in the area can be classified into four categories: hydrothermal type, skarn type, porphyry type, and alkaline granite type rare earth deposits [32–43].

Using the above AHP, a contour map of the comprehensive information value in the working area has been generated, as shown in Figure 3. This map provides crucial information for the delineation of the prospecting target area. By comparing the information values of the known mineralized areas, the lower limit of the comprehensive information value for the prospecting target area can be determined to be 35.

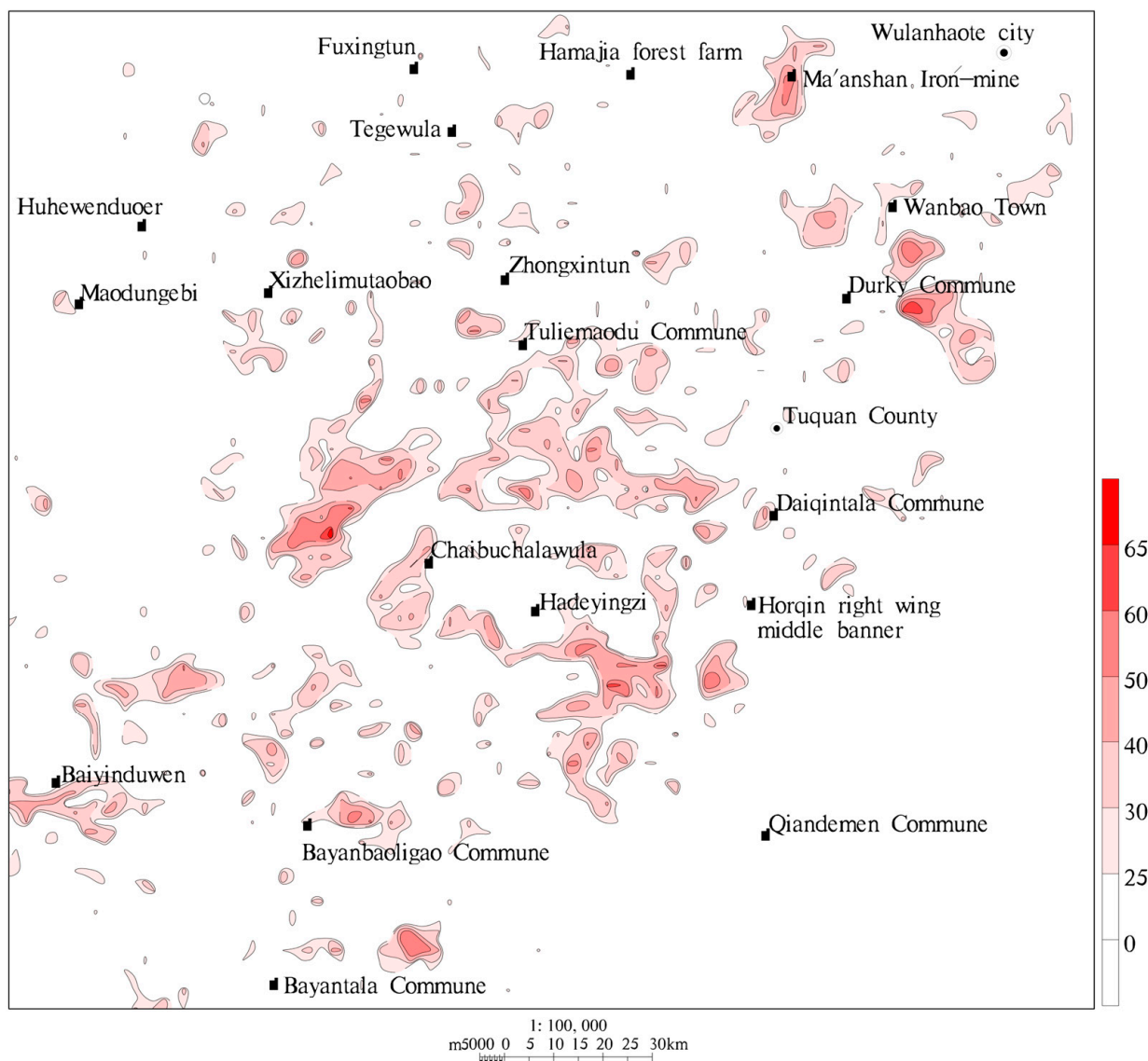


Figure 3. Work area comprehensive information isoline map.

This paper takes the optimization of the multi-metal prospecting target area for the Naoniushan copper–iron polymetallic deposit as an example for a detailed explanation. The area is located in the southeast of the central–southern part of the Great Xing’an Range, approximately 15 km west of Wanbao Town, Tuquan County, Hinggan League, and Inner Mongolia Autonomous Region. Geologically, it is located on the side of the tilted uplift of the boundary between the Wanbao–Mangniu Sea Depression and the Yema Uplift Zone, which turns from north–south to east–west. The area has developed fault structures, mainly in the northeast and northwest directions, similar to those of the known Lianhuashan copper deposit (a copper-dominated deposit with associated lead, zinc, and silver discovered in the 1980s) [44], as shown in Figure 4.

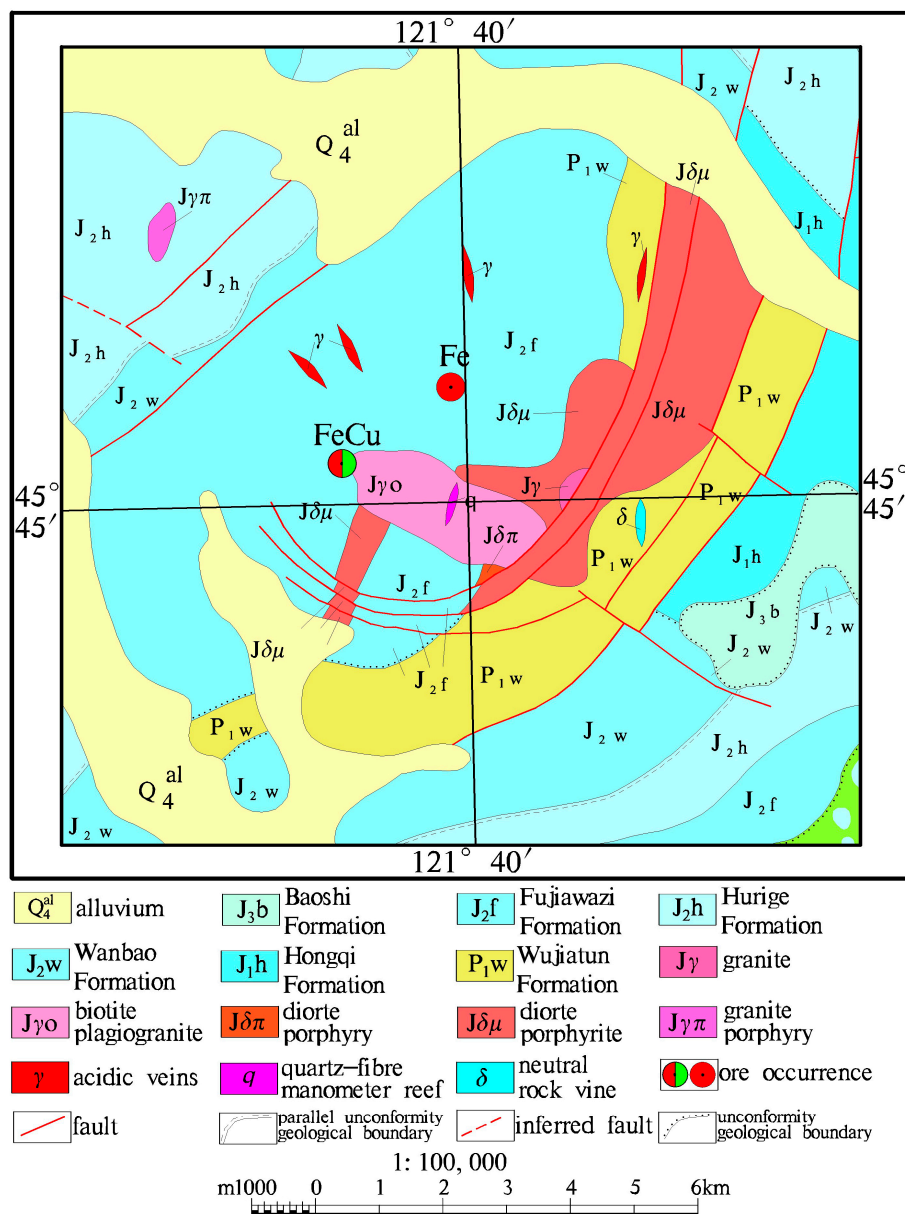


Figure 4. Geological map of the Naoniushan area.

In addition to loose Quaternary sediments, the main stratigraphic units in the area include the following formations: Lower Permian Wujiatun Formation (P_{1w}) sedimentary clastic rock intercalated with limestone lenses; the Middle Jurassic Fujiazhazi Formation (J_{2f}) rhyolite, coarse-grained andesite, and intermediate-acid tuff; the Wanbao Formation (J_{2w}) conglomerate and sandstone intercalated with coal seams; and the Hurihe Formation (J_{2h}) intermediate-acid tuff, tuffaceous conglomerate, and intercalated mudstone lenses. Invasive rock activities are common in the area, and the exposed intrusive rocks mainly consist of diorite porphyrite (J_{δμ}), syenogranite (J_γ), biotite syenogranite porphyry (J_{γo}), diorite porphyry (J_{δπ}), vein-like diorite (δ), granite (γ), and quartz vein (q), etc. Two iron-copper and iron deposits have been discovered in the area, among which the geological environment of the iron-copper deposit is extremely similar to that of the Lianhuashan copper deposit, and both are hydrothermal-porphyry deposits occurring within volcanic structures [45,46].

The regional aeromagnetic anomaly is characterized by the superposition of two north-northeast-oriented medium-weak to medium-strength aeromagnetic anomaly belts on a

smooth and weak negative magnetic field. Two iron–copper and iron deposits have been discovered between the two north–northeast-oriented aeromagnetic anomaly belts. Combined with the geological map, it was observed that the medium–strength aeromagnetic anomaly belt on the southeast side corresponds to diorite porphyrite, diorite porphyry, and granite, and its trend is consistent with the exposed intrusive rocks on the surface. It is inferred that both aeromagnetic anomaly belts are the comprehensive reflection of intermediate-acid intrusive rocks. The geological environment of this area is similar to that of the discovered Lianhuashan medium-sized copper deposit, and the known ore is closely related to the contact alteration. The C-74-215 aeromagnetic anomaly is located within the Jurassic conglomerate and Quaternary sedimentary layers. The maximum anomaly intensity reaches 1400 nT, as shown in Figure 5. The physical property data analysis shows that neither of them can generate such a strong aeromagnetic anomaly. It is inferred that the anomaly is caused by the hidden intermediate-acid intrusive rock and the alteration of the surrounding rock. The location of the ore deposit closely resembles that of the Lianhuashan copper deposit. It is worth noting that the magnetic field in this area exhibits volcanic structure characteristics: the main volcanic vent is located where the granite porphyry body next to the iron-copper deposit is located, corresponding to a weak negative magnetic anomaly on the magnetic field map. This suggests that it may be a product that penetrated along the main volcanic vent. Four medium–strong magnetic anomalies are distributed outward along the main volcanic vent, most of which are indicative of diorite porphyrite, and two are visible on the surface as diorite porphyrite in the south. It is inferred that they could be the products of small vents penetrating and erupting along the arc-shaped fault zone around the main volcanic vent. The andesitic volcanic debris of the Fujiazhazi Formation on the periphery may represent products from the early stage of the volcanic eruption.

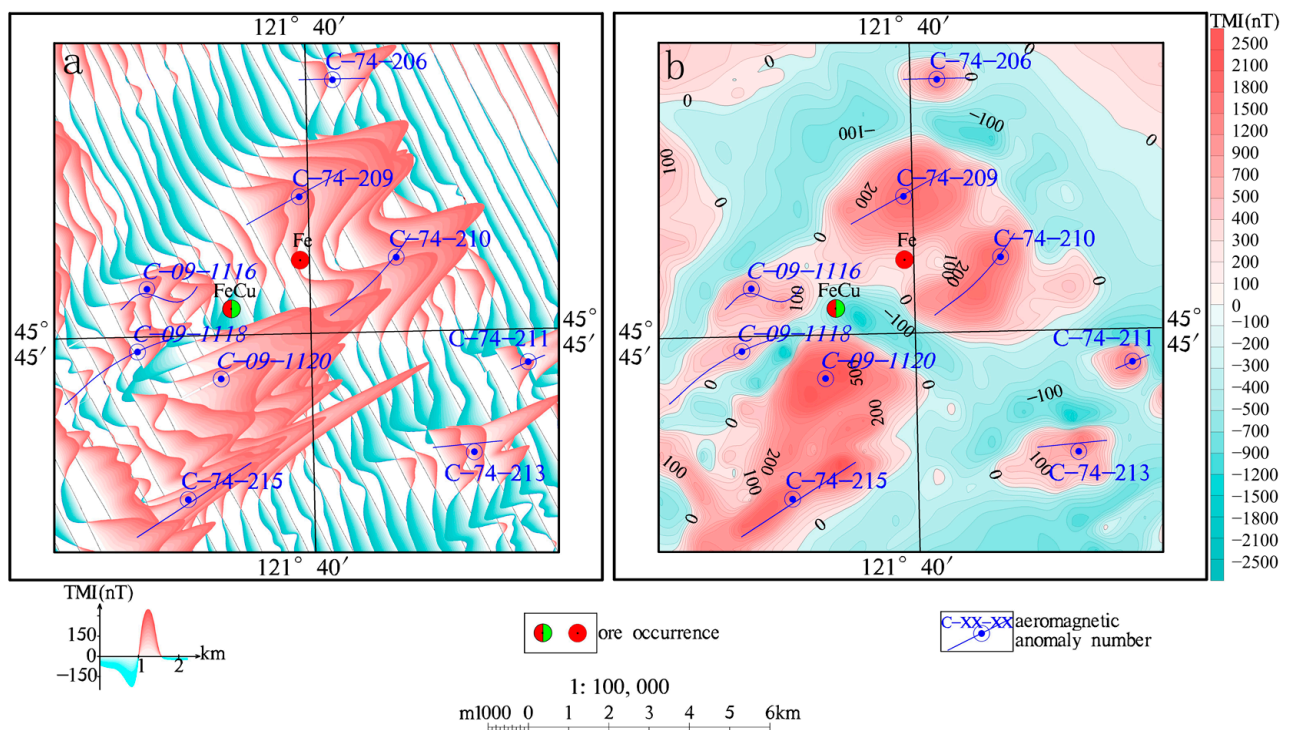


Figure 5. Aeromagnetic total magnetic intensity (TMI) map of the Naoniushan area. (a) Profile map; (b) Contour map.

The airborne electromagnetic field map reveals that apart from the northeast and southwest of the target area, where notable airborne electromagnetic response anomalies are observed, the majority of the other areas are dominated by smooth and low background

fields. Compared with the geological map, the two areas in the northeast and southwest are both Quaternary loose sediments with low resistivity. When they contain a certain amount of water, their resistivity can drop to several ohms, which is the most obvious response on the three-component map of the airborne electromagnetic method, such as the ultra-low-resistive electromagnetic response feature observed in the northeast. Therefore, the resistivity difference of shallow geological bodies in the target area is not significant, and they are all high-resistance bodies, and favorable airborne electromagnetic anomalies for mineralization have not been optimized.

The contour map of the total channel of airborne gamma-ray spectrometry shows that the reflectivity of rocks in the area is relatively low, typically appearing as a zone with a low gamma-ray spectrometry value. The Quaternary and Permian correspond to relatively low levels of radioactive nuclide content. In contrast, the Jurassic and intermediate-acid intrusive rocks correspond to relatively high levels of reflective nuclide content, with small differences between them. As a result, favorable airborne gamma-ray spectrometry anomalies for mineralization have not been optimized within the target area, as shown in Figure 6.

Most areas in the region have comprehensive geochemical anomalies of elements such as Cu, Pb, Au, and As. Specifically near the known ore deposits, there are geochemical anomalies of elements such as Cu, Pb, Au, Ag, and As, with the Cu element representing a high-value geochemical anomaly area. Upon analyzing the geochemical anomaly map, it becomes evident that the known ore deposits near them display a typical geochemical anomaly mineralization pattern of copper and polymetallic ores: a large area of frontal element geochemical anomalies with relatively high concentrations of As, Au, Ag, etc., and low to medium value anomalies of ore-forming elements such as Cu, Pb, and Zn. In addition, within the high-value Au element anomaly area in the southern part of the target area, there are also low-value geochemical anomalies of elements such as Cu, Ag, and Mo. These comprehensive anomaly areas serve as crucial prospecting areas for copper-polymetallic deposits and act as direct indicators for prospecting activities, as shown in Figure 7.

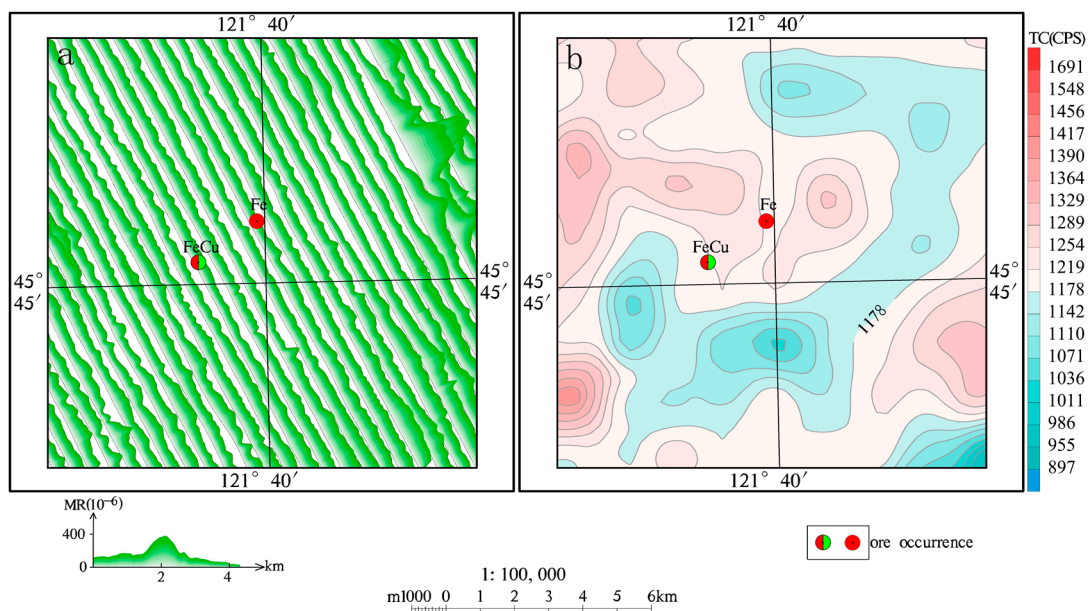


Figure 6. Airborne electromagnetic and airborne radiometric map of the Naoniushan area. (a) Airborne electromagnetic profile map; (b) Contour map of total counts.

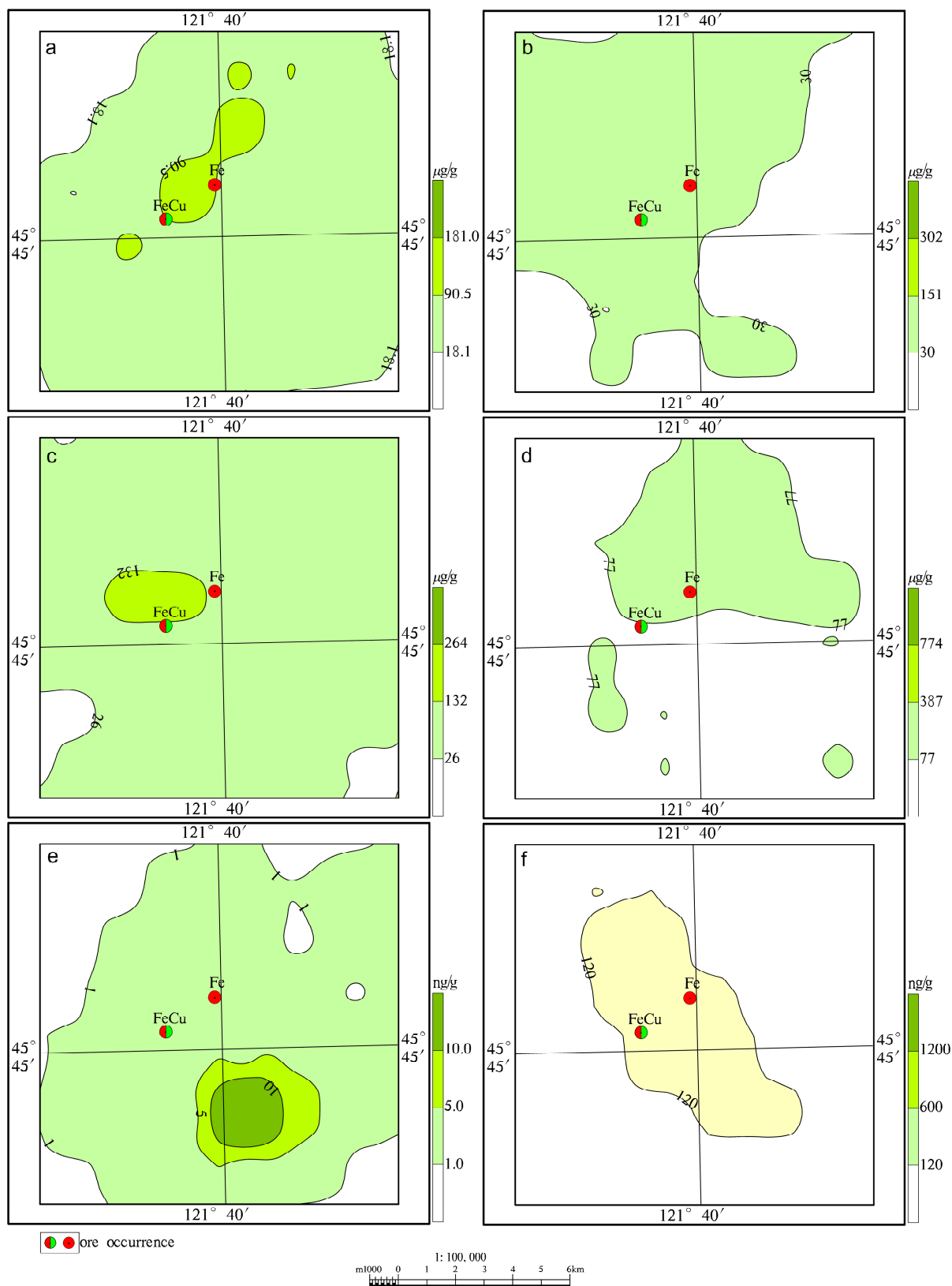


Figure 7. Contour map of geochemical anomalies in the Naoniushan area. (a) Cu; (b) Pb; (c) As; (d) Zn; (e) Au; (f) Ag. The unit above the color scale is $\mu\text{g/g}$, which represents 10^{-2} .

Based on the prospecting indicators mentioned above and referring to Table 1 for the superposition calculation of the information value of each prospecting indicator, a

contour map of comprehensive information value is obtained (as shown in Figure 8). The information value ranges from 25 to 50, and according to the minimum value of 35 determined as the information value threshold for the first-level prospecting division across the entire region of the middle and southern sections of the Daxinganling Mountains, this particular area can be delineated as a prospecting target area.

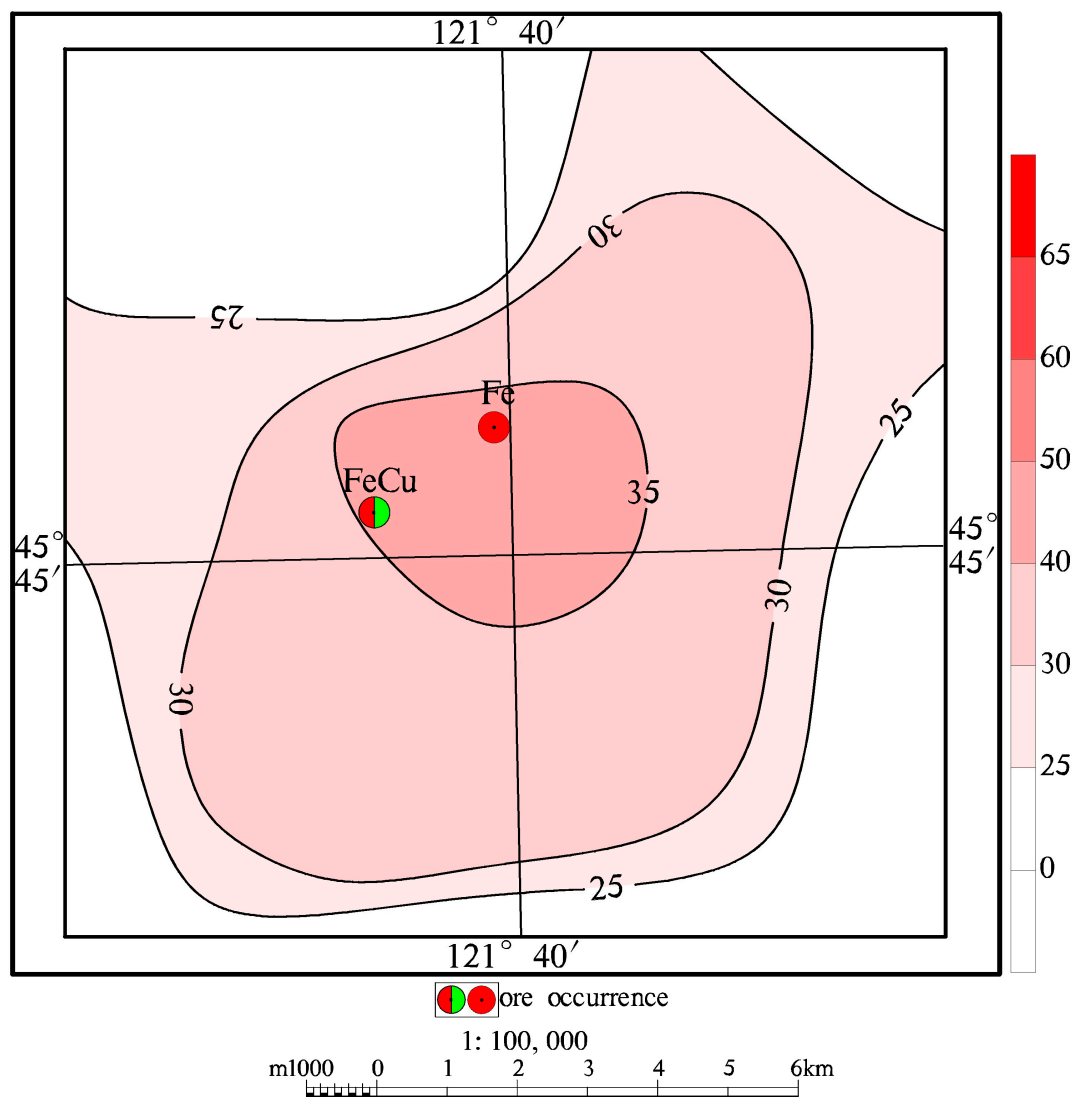


Figure 8. Contour map of the comprehensive information content of copper polymetallic ore prospecting target area in Naoniushan area. The isoline values are dimensionless data.

5. Conclusions

1. This paper has successfully constructed an evaluation system for mineralization target areas based on the principles of the AHP. The weights of each prospecting indicator were calculated, and a comprehensive geological–aerogeophysical–geochemical information value evaluation model was formulated. Various information value weighting methods were developed to suit the characteristics of airborne geophysical exploration. The result is an intuitive contour map of comprehensive information value, providing a systematic theoretical method for optimizing mineralization target areas and conducting objective and comprehensive evaluations.
2. This paper presents an application example of the evaluation system constructed using AHP to select mineralization target areas in the central–southern segment of the Daxinganling region, with a detailed description focusing on the Naoniushan area. An

information content contour map of the study area was generated (Figure 3). Based on the information content values corresponding to known mineral occurrences within the area, a lower threshold value of 35 was determined for identifying prospective mineralization areas. Subsequent field surveys confirmed the effectiveness of this approach, as the identified target areas closely matched the priority exploration zones. A total of 19 prospective target areas have been identified for copper-polymetallic deposits, copper–iron deposits, molybdenum deposits, and lead-zinc deposits in this area. The main types of mineralization include hydrothermal deposits, porphyry deposits, mesothermal hydrothermal deposits, and skarn deposits.

3. The AHP method has limitations related to data richness and interpreter understanding. It also has a certain time limit. As geological, geophysical, and geochemical technologies continue to develop and improve, along with the enrichment of various information values and the improvement of measurement accuracy, as well as the improvement of the interpreter's understanding, the evaluation results are not immutable and can evolve over time.
4. The methods presented in this paper pertain to predicting prospective mineralization areas in reconnaissance exploration projects that utilize airborne geophysical data. However, when conducting surveys targeting specific mineral resources or employing specific methods and technologies in specific regions, the hierarchical models for predicting prospective mineralization areas need to be designed separately to meet the project's requirements, considering the actual circumstances.

Shallow ore prospecting has become increasingly challenging, requiring deeper exploration and more complex mineralization predictions. Continuous innovation in prospecting ideas and prediction methods is necessary. With the continuous development of technology, big data and artificial intelligence have revolutionized the field of earth science in recent years. These advancements push for a shift from traditional qualitative and combined qualitative–quantitative geological research towards quantitative research, providing new ideas for future quantitative prediction of prospecting targets using big data.

Author Contributions: Conceptualization, Y.X., G.L., Y.L. and N.L.; methodology, Y.X. and G.L.; software, Y.X.; investigation and validation, Y.X. and G.L.; writing—original draft preparation, Y.X. and N.L.; writing—review and editing, all participants; supervision, G.L., J.L., Q.W. and S.W. All authors have read and agreed to the published version of the manuscript.

Funding: This research was funded by the Basic Scientific Research Project of the Chinese National Nonprofit Institute (grant number AS2022J01).

Data Availability Statement: Not applicable.

Acknowledgments: We are thankful for the constructive comments of the editors and anonymous reviewers that improved this paper. We are also grateful for the help from Qing-Min Meng, Zhi-Qiang Cui, and Wei-Dong Gao in data acquisition and system development.

Conflicts of Interest: The authors declare no conflict of interest.

References

1. Zhao, Z.Y.; Chen, H.G.; Pan, M.; Jia, G.; Li, X.Q.; Xu, S.Y.; Guo, G.; Zhang, X.Y. Application of the weighted logistic regression model in prediction of volcanic rock-hosted copper deposits-taking the middle part of Ning-Wu basin as an example. *Geol. J. China Univ.* **2016**, *22*, 105–112.
2. Bai, H.; Cao, Y.; Zhang, H.; Wang, W.; Jiang, C.; Yang, Y. Applying Data-Driven-Based Logistic Function and Prediction-Area Plot to Map Mineral Prospectivity in the Qinling Orogenic Belt. *Cent. China Miner.* **2022**, *12*, 1287. [[CrossRef](#)]
3. Zhao, J.; Sui, Y.; Zhang, Z.; Zhou, M. Application of Logistic Regression and Weights of Evidence Methods for Mapping Volcanic-Type Uranium Prospectivity. *Minerals* **2023**, *13*, 608. [[CrossRef](#)]
4. Li, S.; Liu, C.; Chen, J. Mineral Prospecting Prediction via Transfer Learning Based on Geological Big Data: A Case Study of Huayuan, Hunan, China. *Minerals* **2023**, *13*, 504. [[CrossRef](#)]
5. Zuo, R.G. Identification of high prospective terrains by comprehensive evaluation based on multilevel fuzzy synthesis judgment. *Geol. Explor.* **2009**, *45*, 85–89.

6. Liu, Z.J. The application of hierarchical analytical technique to the classification of aeromagnetic anomalies and the ore-prospecting prognosis in central and western Qinghai—Tibet plateau. *Geophys. Geochem. Explor.* **2001**, *25*, 161–168.
7. Zhao, P.D. *The Theory and the Method for Mineral Resource Exploration*; China University of Geosciences: Wuhan, China, 2001.
8. Fan, Y.X.; Yang, Z.X. *Metallogenic Regularity and Metallogenic Prediction*; China University of Mining and Technology: Beijing, China, 2003.
9. Qi, W.T.; Muhetaero, Z.R.; Wu, T.W.; Zhang, K.; Liu, X.L. Analytic hierarchy process for optimum target areas in mineral resource prospecting. *Met. Mine* **2012**, *433*, 106–109.
10. Wang, Y.J.; Li, M.S.; Quan, X.D.; Ma, M.T.; Ma, X.H. Application of GIS-based analytic hierarchy process for min-erogenetic prediction. *Geol. Sci. Technol. Inf.* **2007**, *26*, 15–18.
11. Wang, Y.J.; Li, M.S.; Ma, M.T.; Wang, B. Application of analytic hierarchy process for uranium deposits prediction in north Tarim basin. *Geol. Sci. Technol. Inf.* **2009**, *28*, 71–74.
12. Hao, B.W. AHP and multiple-grade fuzzy evaluation (MG-FE) coupling modle based on comprehend-sive informa-tion for metallogenic prediction to the Puqing antimaony—Gold orefield in Guizhou Province. *Geol. Explor.* **2010**, *46*, 741–750.
13. Lu, H.X.; Wang, Y.J.; Wang, B.; Zhang, E.; Wang, R.J.; Li, M.S. Application of GIS-based analytic hierarchy process for uranium minerogenetic prediction in Guyuan region. *Adv. Earth Sci.* **2014**, *8*, 968–973.
14. Zhou, K.F.; Zhang, N.N. Mineral prospectivity mapping for porphyry-type and hydrothermal vein-type copper deposits using fuzzy analytical hierarchy process and geographic information system. *J. Intell. Fuzzy Syst.* **2016**, *31*, 3143–3153. [[CrossRef](#)]
15. Shabani, A.; Ziaii, M.; Monfared, M.S.; Shirazy, A. Multi-Dimensional Data Fusion for Mineral Prospectivity Mapping (MPM) Using Fuzzy-AHP Decision-Making Method, Kodegan-Basiran Region, East Iran. *Minerals* **2022**, *12*, 1629. [[CrossRef](#)]
16. Liu, C.; Wang, Y.T.; Chen, A.J. Application of AHP in the predication of mineral resources by comprehen-sive information. *J. Chang. Univ. Earth Sci.* **1994**, *24*, 222–228.
17. Saaty, T.L.; Kearns, K.P. Systems Characteristics and The Analytic Hierarchy Process. In *The Analytic Hierarchy Process*; Saaty, T.L., Kearns, K.P., Eds.; Analytical Planning; Elsevier: Amsterdam, The Netherlands, 1985; pp. 63–86.
18. Li, Q.N.; Zhao, Q.N.; Nie, Y. Research on the Factors Affecting the Development of Wind Power Industry Based on Analytic Hierarchy Process(AHP)—Taking Jiuquan Wind Power Generation Base in Gansu Province as an Example. *Power Syst. Clean Energy* **2019**, *10*, 75–81.
19. Wang, X.H.; Liu, H.F.; Ji, H.L.; Wang, Z.Y.; Wang, E.Q.; Pang, J.J.; Shao, A.L. Screening test of fine varieties of peony cut flowers based on analytic hierarchy process. *Shaanxi J. Agric. Sci.* **2020**, *66*, 36–40.
20. Hu, X.L.; Wang, Y.Z. Application of Analytic Hierarchy Process (AHP) in evaluation of demonstra-tion rivers and lakes. *Water Resour. Dev. Manag.* **2020**, *9*, 77–81.
21. Zhao, Q. Construction of the Comprehensive Quality Evaluation System of College Students Based on AHP. *J. Univ. Shanghai Sci. Technol.* **2023**, *45*, 107–112.
22. Taheri, K.; Thomas, M.M.; Taheri, M.; Moayed, H.; Pour, F.M. Critical Zone Assessments of an Alluvial Aquifer System Using the Multi-influencing Factor (MIF) and Analytical Hierarchy Process (AHP) Models in Western Iran. *Nat. Resour. Res.* **2020**, *29*, 1163–1191. [[CrossRef](#)]
23. Numata, M.; Sugiyama, M.; Mogi, G. Barrier Analysis for the Deployment of Renewable-Based Mini-Grids in Myanmar Using the Analytic Hierarchy Process (AHP). *Energies* **2020**, *13*, 1400. [[CrossRef](#)]
24. Mulu, M.T.; Bitew, M.A.; Tadesse, W.A. Flood Hazard Zoning of Upper Awash River Basin, Ethiopia, Using the Analytical Hierarchy Process (AHP) as Compared to Sensitivity Analysis. *Sci. World J.* **2023**, *2023*, 1675634.
25. Van, N.T.A.; David, T.; Tan, P.N. Indicators for TQM 4.0 model: Delphi Method and Analytic Hierarchy Process (AHP) analysis. *Total Qual. Manag. Bus. Excell.* **2023**, *34*, 220–234.
26. Issan, K.; Hedia, C.; Youssouf, K.; Kamel, Z. Assessment of Aquifer Recharge Potential Using Remote Sensing, GIS and the Analytical Hierarchy Process (AHP) Combined with Hydrochemical and Isotope Data (Tamassari Basin, Burkina Faso). *Water* **2023**, *15*, 650.
27. Zhou, J.; Tan, S.; Li, J.; Xu, J.; Wang, C.; Ye, H. Landslide Susceptibility Assessment Using the Analytic Hierarchy Process (AHP): A Case Study of a Construction Site for Photovoltaic Power Generation in Yunxian County, Southwest China. *Sustainability* **2023**, *15*, 5281.
28. Gavhane Kishor, P.; Kumar, M.A.; Arjamadutta, S.; Kumar, S.D.; Susama, S. Targeting of rainwater harvesting structures using geospatial tools and analytical hierarchy process (AHP) in the semi-arid region of Rajasthan (India). *Environ. Sci. Pollut. Res. Int.* **2023**, *30*, 61682–61709. [[CrossRef](#)]
29. Mohammed, R.; Suliman, A.A. Land Suitability Assessment for Wheat Production Using Analytical Hierarchy Process (AHP) and Sys Parametric Method in Babylon Province. *J. Ecol. Eng.* **2023**, *24*, 75–87. [[CrossRef](#)]
30. Ramdhan, O.M.; Aleks, O.; Ririn, P.; Putra, O.M.Y.U. GIS-based analytic hierarchy process (AHP) for soil erosion-prone areas mapping in the Bone Watershed, Gorontalo, Indonesia. *Environ. Earth Sci.* **2023**, *82*, 225.
31. Laura, Z.F.; Nsangou, N.M.; Balla, A.M.C.; Monespérance, M.G.M.; Wabo, D.P.L.; Tetang, K.R.; Kagou, D.A.; Sébastien, O. Landslide susceptibility zonation using the analytical hierarchy process (AHP) in the Bafoussam-Dschang region (West Cameroon). *Adv. Space Res.* **2023**, *71*, 5282–5301.
32. Heilongjiang Geological Bureau. *Regional Geology and Metallogenic Regularity of Daxinganling and Its Adjacent Areas*; Geological Publishing House: Beijing, China, 1959.

33. Niu, S.G.; Guo, L.J.; Wang, B.D.; Sun, A.Q.; Wang, S. Regional tectonic evolution and mineralization in the middle and southern part of Daxinganling. *LiLunYanTao* **2005**, *1*, 44–46.
34. Bai, L.A.; Sun, J.G.; Zhang, Y.; Han, S.J.; Yang, F.C.; Men, L.J.; Gu, A.L.; Zhao, K.Q. Genetic type, mineralization epoch and geodynamical setting of endogenous copper deposits in the Great Xing'an Range. *Acta Petrol. Sin.* **2012**, *28*, 468–482.
35. Wang, Q.Y. Metallogenic characteristics and prospecting direction of copper polymetallic deposits in central and southern Greater Khingan Range. *Prospecting Technol.* **2018**, *20*, 99–101.
36. Su, M.X.; Yang, B.; Wu, Y.J.; Yan, P.; Meng, X.L. Deep mineralization processes in the central—South Great Hinggan magmatic belt. *Geol. Rev.* **2020**, *66*, 1321–1333.
37. Xue, G.; Luo, J.Y. The identification marks of large and medium-sized continental subvolcanic hydrothermal deposits in the middle and southern section of the Greater Khingga Range. *Inn. Mong. Sci. Technol. Econ.* **2011**, *13*, 63–64.
38. Zhang, H.; Wang, X.L.; Liu, D.R.; Sun, Y.Q.; Cheng, M.L. Ore-forming conditions and exploration potential of typical Ag-Sn polymetallic deposits in the central-southern Da Hinggan Mountains. *Geol. Explor.* **2021**, *57*, 39–52.
39. Zhang, M.; Zhai, Y.S.; Shen, C.L.; Liu, Y.H.; Yang, S.S.; Zhai, D.G.; Yao, M.J.; Wang, J.P.; Wang, S.G.; Gao, Z.X.; et al. Metallogenic system of copper polymetallic deposits in the middle-southern part of Da Hinggan Mountains, Chian. *Geoscience* **2011**, *25*, 819–831.
40. Wang, J.B.; Wang, Y.W.; Wang, L.J. Copper metallogenic setting and prospecting potential in the middle-southern part of Da Hinggan Mountains. *Geol. Prospect.* **2000**, *36*, 1–4.
41. Zeng, Q.D.; Liu, J.M.; Li, B.Y.; Guo, L.J. Types of tin polymetallic mineralization in the middle-southern section of Da Hinggan Mountains. *Acta Mineral. Sin.* **2015**, 96–97.
42. Zhang, Z.; Li, W.; Liu, J.M.; Zeng, Q.D. Progress of exploration and prospecting thoughts for silver polymetallic deposit at southern-middle parts of the Da Hinggan Mountains. *Gold Sci. Technol.* **2016**, *24*, 60–65.
43. Du, Q.S.; Li, Z.H.; E, A.Q.; Yao, Z.W. Geological characteristics and genesis of skarn type lead-zinc deposit in the central-southern Daxinganling belt. *Miner. Explor.* **2017**, *8*, 366–373.
44. Kang, H.; Liu, Y.F.; Jiang, S.H. Molybdenite Re-Os dating and ore S-Pb isotopes of the Lianhuashan Cu deposit, Inner Mongolia, and their genetic significance. *Acta Geol. Sin.* **2019**, *93*, 3082–3094.
45. The Second Comprehensive Geophysical Exploration Brigade of the Ministry of Geology and Mineral Resources. *1/200000 Regional Geological Survey Report and Mineral Map of Tuquan Sheet (L-51-20)*; National Geological Archives of China: Beijing, China, 1983.
46. Geng, W.H.; Yao, J.Y. Metallogenic background of the Naoniushan copper deposit, east inner Mongolia. *Miner. Resour. Geol.* **2004**, *18*, 240–244.

Disclaimer/Publisher's Note: The statements, opinions and data contained in all publications are solely those of the individual author(s) and contributor(s) and not of MDPI and/or the editor(s). MDPI and/or the editor(s) disclaim responsibility for any injury to people or property resulting from any ideas, methods, instructions or products referred to in the content.